Materials Research, Vol. 7, No. 1, 35-41, 2004.

Oxygen-Induced Intergranular Fracture of the Nickel-Base Alloy IN718 during Mechanical Loading at High Temperatures

Ulrich Krupp[a]*, *William Kane*[b], *Jeffrey A. Pfaendtner*[c], *Xinyu Liu*[b]
Campbell Laird[b], *Charles J. McMahon Jr.*[b]

[a]*Institut für Werkstofftechnik, Universität Siegen, 57068 Siegen, Germany*
[b]*Department of Materials Science and Engineering, University of Pennsylvania, 3231 Walnut Street, PA19104, Philadelphia, U.S.A.*
[c]*General Electric Aircraft Engines, 1 Neumann Way, OH45215, Cincinnati, U.S.A.*

Received: September 2, 2002; Revised: September 4, 2002

There is a transition in the mechanical-failure behavior of nickel-base superalloys from ductile transgranular crack propagation to time-dependent intergranular fracture when the temperature exceeds about 600 °C. This transition is due to oxygen diffusion into the stress field ahead of the crack tip sufficient to cause brittle decohesion of the grain boundaries. Since very high cracking rates were observed during fixed-displacement loading of IN718, it is not very likely that grain boundary oxidation governs the grain-boundary-separation process, as has been proposed in several studies on the fatigue-damage behavior of the nickel-base superalloy IN718. Further studies on bicrystal and thermomechanically processed specimens of IN718 have shown that this kind of brittle fracture, which has been termed "dynamic embrittlement", depends strongly on the structure of the grain boundaries.

Keywords: *IN718, intergranular fracture, dynamic embrittlement, grain boundary diffusion*

1. Introduction

Polycrystalline nickel-base superalloys commonly used for high-temperature, high-strength components in gas turbines, in particular turbine discs, show a significant change in the failure mechanism when loaded slowly at high temperatures above 600 °C. Instead of cycle-dependent fatigue crack propagation by plastic blunting and/or power-law creep, the time-dependent diffusion of atmospheric oxygen into the grain boundaries (GBs) under the influence of tensile stress causes brittle intergranular fracture, which has been observed in numerous studies (e.g.[1-5]). Certainly, this kind of fast crack propagation is undesirable during operation of high-temperature components, and therefore a great deal of effort has been spent by several researchers to improve the resistance of the grain boundaries against the attack of oxygen, e.g., by enlarging the grain size[6], by the addition of grain boundary strengtheners (e.g. B, Zr, Hf, C)[7] or by grain boundary engineering (GBE)[8], a thermomechanical treatment to increase the fraction of special GBs, which might exhibit a lower oxygen GB diffusivity.

*e-mail: krupp@ifwt.mb.uni-siegen.de
Presented at the International Symposium on High Temperature Corrosion in Energy Related Systems, Angra dos Reis - RJ, September 2002.

2. Grain Boundary Oxidation

The combination of high tensile stresses and high temperatures facilitates the ingress of oxygen by grain boundary diffusion, which might be followed by grain-boundary oxidation – a mechanism that has been termed as SAGBO (stress-accelerated grain-boundary oxidation[7,9]). If the kinetics of oxide formation are sufficient, fast intergranular crack propagation is governed by the brittle fracture of oxidation products supported by creep cavitation in the high-stressed damage zone ahead of the crack tip. This was shown in earlier studies as to be a typical failure mechanism during low-cycle fatigue (LCF) of gas turbine blades[10]. For intergranular failure at moderate temperatures, typically in the range between 600 °C and 700 °C, Molins *et al.*[4] and Andrieu *et al.*[11] proposed a grain boundary cracking mechanism that involves the formation of NiO nuclei at the fresh fracture surface. The removal of Ni cations leads to the injection of vacancies that cannot be annihilated because of the initial epitaxial oxide growth. The accumulation of vacancies ahead of the crack tip is assumed to promote brittle grain boundary fracture. In addition to this, initial oxida-

tion of Ni leads to a near-surface diffusion zone in which the Cr concentration has exceeded its initial value. As long as no Cr-containing oxide is formed (by which Cr would be consumed), this Cr-enriched diffusion zone contributes to the brittle behavior of the grain boundaries during mechanical loading. Their assumptions were supported by LCF experiments on model alloys containing different initial Cr concentrations, as well as at different oxygen partial pressures. There is obviously a transition pressure below which no brittle fracture occurs, which is about 10^{-3} Pa for pure Ni and about 10^{-1} Pa for Ni with 20 wt.% Cr (IN718).

3. Dynamic Embrittlement

Oxygen-induced intergranular fracture does not necessarily require the formation of oxides. At temperatures around 650 °C, oxidation kinetics of chromia- or alumina-forming Ni-base superalloys are fairly slow. As an alternate mechanism, dynamic embrittlement can cause intergranular failure at high cracking rates. This mechanism involves the diffusion of an adsorbed element into a grain boundary under the influence of a tensile stress, similar to the Hull-Rimmer mechanism[12], which describes the growth of creep cavities by the diffusion of atoms from the cavity surface into the surrounding GB. The embrittling atoms in the GB can lower the cohesion of the atomic bonds, which will finally break under the influence of the tensile stress. Figure 1 illustrates schematically this kind of time-dependent damage mechanism. Dynamic embrittlement was shown to cause intergranular failure for several alloys and different embrittling species in earlier studies, e.g., sulfur-induced cracking of alloy steels[13], tin-induced cracking of Cu-Sn alloys[14] and oxygen-induced cracking of a Cu-Be alloy[15], of a Ni-Mo-Cr alloy[16], and of the intermetallic alloy Ni_3Al[17]. In a more recent study, intergranular brittle fracture during static loading of IN718 has been attributed also to dynamic embrittlement[8,18].

The driving force for GB diffusion is (beside the concentration gradient) the tensile stress σ acting ahead of the crack tip, which reduces the chemical potential of the atoms by $\Delta\mu = -\Omega\sigma$ when they are moved from the free surface into the grain boundary. Adding the diffusive flux driven by a stress gradient to the diffusion differential equation (Ficks's 2nd law) one gets the following governing equation for dynamic embrittlement:

$$\frac{\partial c}{\partial t} = D_b \frac{\partial^2 c}{\partial x^2} - \frac{D_b \Omega}{kT} \frac{\partial}{\partial x}\left(c \frac{\partial \sigma}{\partial x} \right) \qquad (1)$$

where D_b is the grain-boundary diffusivity, Ω is the atomic volume, k is the Boltzmann constant, and T is the absolute temperature. This equation has been used to describe oxygen-induced intergranular cracking quantitatively by a steady state model by Xu and Bassani in[19] that takes elastic and plastic (creep) deformation within the cohesive zone ahead of the crack tip into consideration. By applying to tin-induced intergranular fracture of Cu-Sn bicrystals, this model yielded a penetration depth of the embrittler in a sufficient concentration for cracking in the order of 10^{-9}m. Thus, short-range grain boundary diffusion does govern the dynamic embrittlement process, which is in agreement with the fairly high cracking rates that have been observed experimentally.

4. Experimental Procedures

Mechanical and oxidation testing were done on specimens of the nickel-base superalloy IN718, a chromia-forming material strengthened by the ordered fcc γ' phase with a volume fraction of approx. 30%-35% and the bct γ'' phase

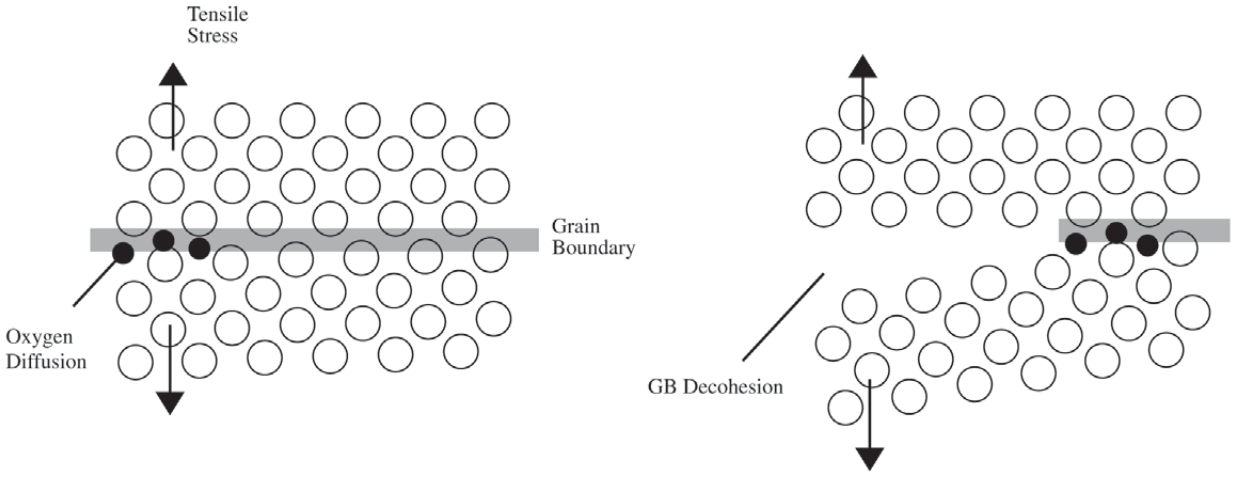

Figure 1. Schematic representation of the dynamic-embrittlement mechanism.

after solution heat treatment at 1050 °C (1h) followed by aging at 720 °C (12h) and 620 °C (12h). The chemical composition is given in Table 1.

Some sheets of this "as-received" material were thermomechanically processed by 20% cold-rolling followed by annealing at 1050 °C (1h), a sequence that was applied four times to the material which was then termed "grain boundary engineered (GBE)". The mean diameter of the as-received as well as of the GBE specimens was about 74 µm.

A third group of specimens was produced by diffusion bonding of polished IN718 single crystals with a certain crystallographic relationship in a vacuum furnace at 1050 °C for 100 h and a compression stress of $\sigma \approx 10$ MPa. The bicrystals made by this method were elongated by brazing two small polycrystalline IN718 blocks onto the surfaces parallel to the grain boundary (Fig. 2b).

Single-edge-notched bending specimens (SENB) having a geometry as shown in Fig. 2a were cut by electro-discharge machining (EDM). To obtain reproducible conditions, the root of the notch was either polished by a 100 µm diameter Mo wire that was drawn back and forth through the notch using 3 µm diamond paste or extended by fatigue precracking.

Four-point-bending tests were carried out in a high-vacuum-tight chamber originally designed and built by Pfaendtner in an earlier study[18] in which the specimen are heated by 750W infrared lamps focussed through quartz glass windows onto the center area of the bending specimens. The experimental setup is shown in Fig. 2c. Crack propagation was studied by (1) loading the specimens to a certain maximum load and then (2) keeping the displacement fixed. The following load drop was recorded as a function of the time and corresponds with the crack propagation, which was determined by calibration curves[8,18].

Most of the microstructural examinations were done using analytical scanning electron microscopy (SEM). To determine the distribution of the crystallographic orientations within the microstructure, orientation-imaging microscopy (OIM)^TM was applied to electropolished specimens in the SEM. This technique is based on the diffraction of back-scattered electrons, yielding sets of Kikuchi patterns for each local orientation.

To obtain information about the isothermal-oxidation behavior of IN718, some continuous and discontinuous thermogravimetric measurements have been carried out.

5. Results and Discussion

There is no general description of the oxidation of Ni-base superalloys at temperatures of about 650 °C. At high temperatures overall oxidation kinetics are determined after a short time by the growth of the most protective and stable oxide (i.e., Cr_2O_3 or Al_2O_3). At moderate temperatures, where diffusion becomes much slower, oxidation depends on additional processes and interfacial reactions, e.g., vacancy injection into the metal matrix during the growth of p-type oxides (cation vacancies in the oxide scale)[11].

Table 1. Chemical composition of the Ni-base superalloy IN718.

Ni	Fe	Cr	Nb	Mo	Ti	Al	Co	Si	Mn	C	B
Bal.	18.7	18.2	5.2	3.0	1.0	0.5	0.1	0.4	0.06	0.04	0.004

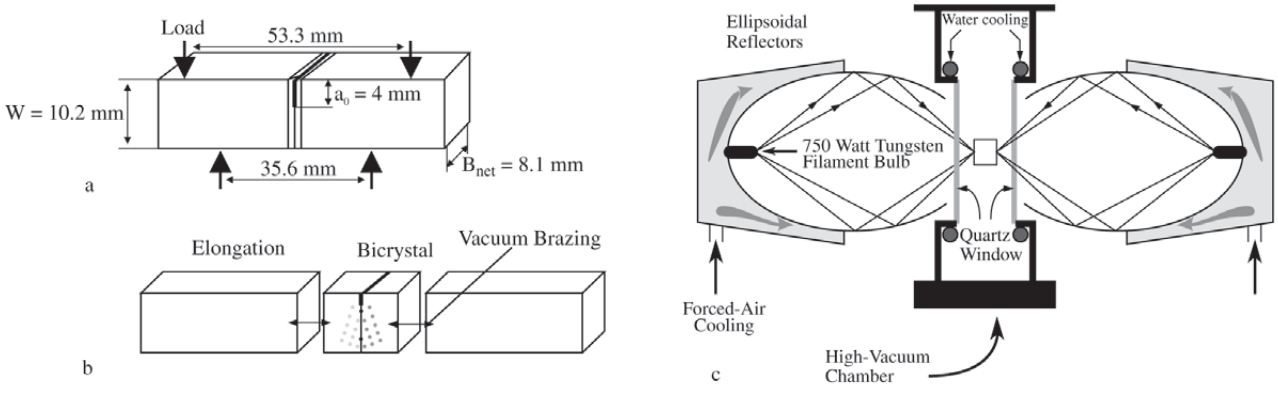

Figure 2. a-b) Specimen geometry; c) experimental setup.

The oxidation of IN718 at lower temperatures is determined by the preferential oxidation of niobium and titanium carbides[20] and the formation of $(Cr,Fe)_2O_3$ and $FeNbO_4$[21]. Contrary to these results Diboine and Pineau[22] found that the initial oxidation behavior of IN718 at 650 °C is determined by a preferential Cr_2O_3 formation in the vicinity of GBs. Figure 3a shows the thermogravimetrically-determined kinetics of the oxidation process at 650 °C in air. The initial oxidation process obeys a linear rate law rather than a parabolic one, due to non-protective partial coverage of the metal surface by oxidation products, mainly oxidized niobium carbides (Fig. 3b). While at 850 °C a pronounced chromia formation at the GBs could be observed, there is no preferential GB oxidation at 650 °C. A parabolic rate constant (k_p''= $(m/A)^2/t$) for oxidation at 650 °C was estimated as k_p''(650) = $5.8\times10^{-15} g^2cm^{-4}s^{-1}$ which is by two orders of magnitude lower than the one for oxidation at 850 °C k_p''(850)=$3.4 \times 10^{-13} g^2cm^{-4}s^{-1}$.

Figure 4 shows the load *vs.* time curves for cracking of IN718 at 650 °C in dry oxygen. After a certain incubation time, during which an intergranular crack initiates (possibly by power law creep), an intergranular crack grows by a quasi-brittle propagation rate for an initial stress intensity factor of K = 30MPam$^{1/2}$. During fast cracking the chamber

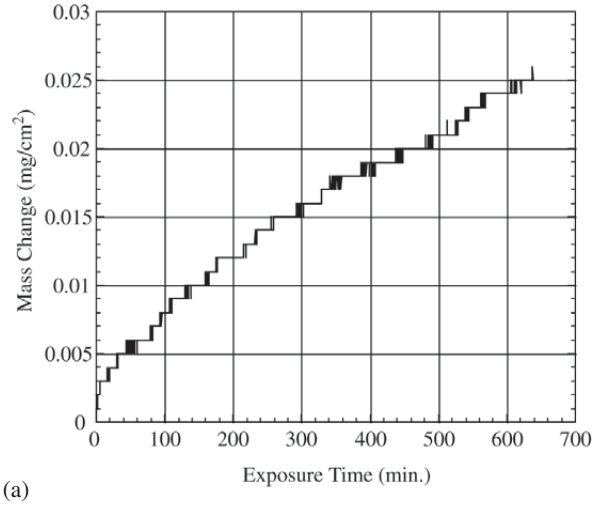

(a)

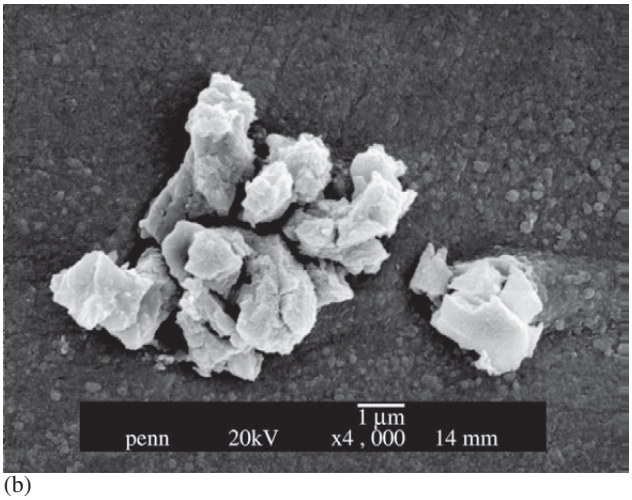

(b)

Figure 3. a) Continuously-measured mass change *vs.* time for the exposure of IN718 at 650 °C to air; b) oxidation products (Nb_2O_5) formed under these conditions on the surface.

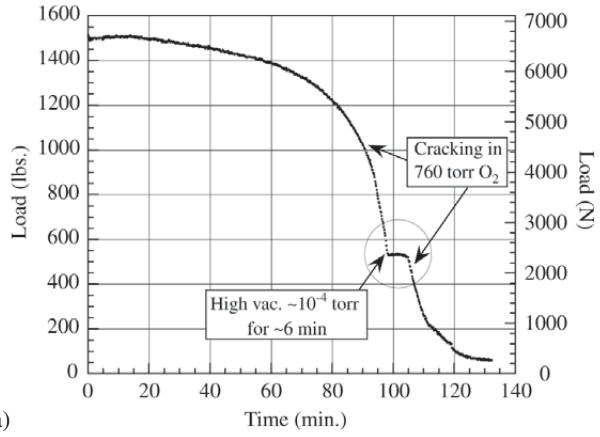

(a)

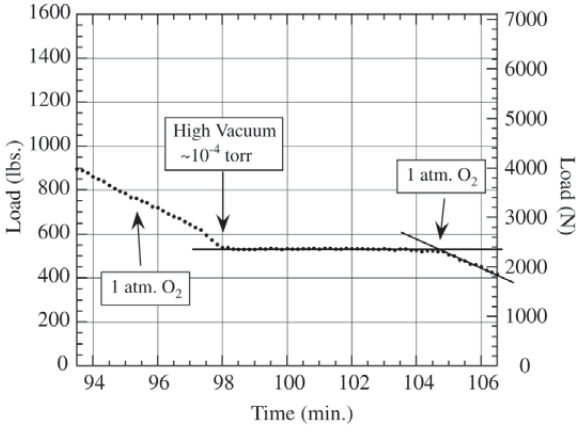

(b)

Figure 4. Cracking of an IN718 4pt-bending specimen (with fatigue precrack) under fixed displacement loading at 650 °C interrupted by evacuating the chamber, b) shows a detail of a) (Ref. [18]).

was pumped for a short time to a high vacuum of $< 10^{-4}$ Torr ($< 1.33 \times 10^{-4}$ mbar). The detail of the load drop *vs.* time curve in Fig. 4b shows that crack propagation can be "switched off" by evacuating the chamber. As soon as the chamber was back-filled with oxygen, cracking resumed within a few seconds.

This experiment supports the proposed dynamic-embrittlement process as the governing mechanism for intergranular failure of Ni-base superalloys. It seems to be not very likely that during the short time between back-filling with oxygen and onset of crack propagation enough vacancies can be generated due to NiO formation, even if the oxidation rate under the influence of stress is higher than the isothermal one that is represented in Fig. 3.

Generally, the fracture surfaces generated during high-temperature 4pt-bending tests consist predominantly of smooth grain-boundary facets showing no evidence of pronounced pore formation or strong plastic deformation. Figure 5 represents the intergranular crack tip after interrupting a fixed-displacement test by abrupt unloading and breaking the remaining cross section by room-temperature impact. The abrupt unloading preserved the fracture surface during the stages of crack advance. Fig. 5 indicates obviously that within a band of approximately 1µm in the crack tip area no oxidation had occurred, while the broken GB left behind is covered with oxidation products.

On the other hand, there is a small fraction of grain boundaries which show pronounced plasticity (Fig. 6a) or which failed by ductile rupture (Fig. 6b). The broken GB depicted in Fig. 6a is interrupted by the terminus of a twin boundary which changes locally the crystallographic orientation relationship. Obviously brittle-crack propagation across this particular GB plane is hindered in the twin-boundary area by a difference in oxygen GB diffusion kinetics for a changed crystallographic misorientation. This hypothesis is supported by the observation of several GBs, which were broken completely by ductile rupture. It is very likely that these GBs were left as unbroken ligaments until the local stress level increased to a value sufficient to cause unstable ductile fracture, which is indicated by dimples in the fracture surface.

There exist some data in the literature which show that

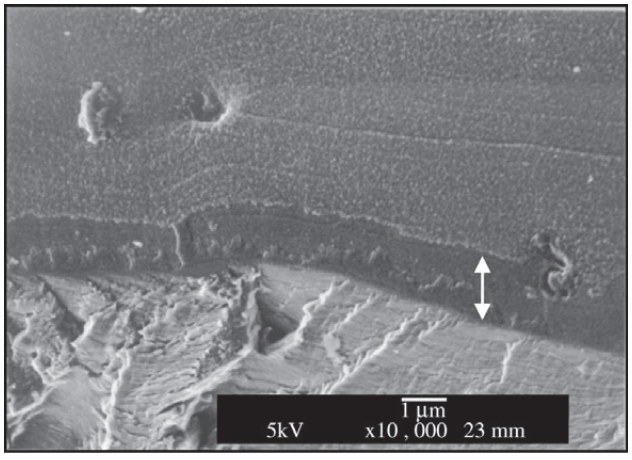

Figure 5. Oxide-free crack tip area with (arrow) in the fracture surface of an IN718 bending specimen loaded under fixed displacement at 650 °C (Ref.[18]).

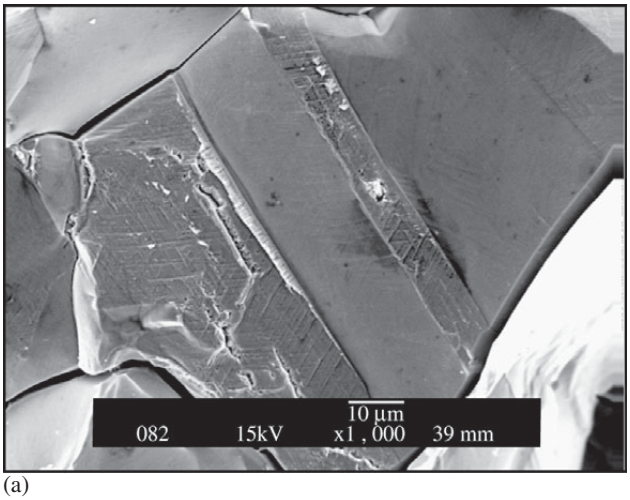

(a)

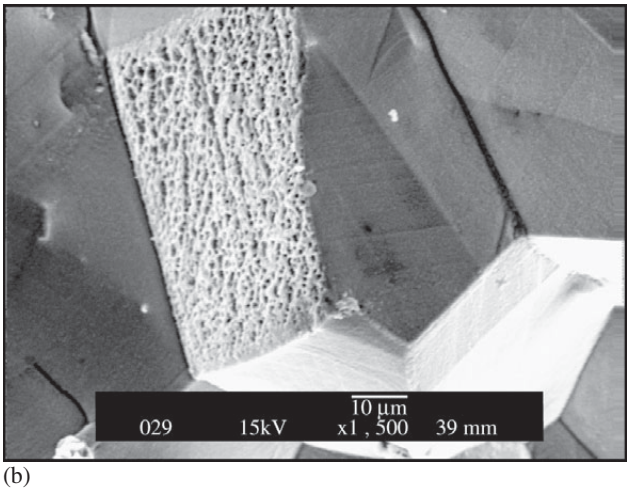

(b)

Figure 6. Fracture surface of IN718 4pt-bending specimens loaded under fixed displacement at 650 °C: a) terminus of a twin boundary; b) grain boundary broken by ductile rupture.

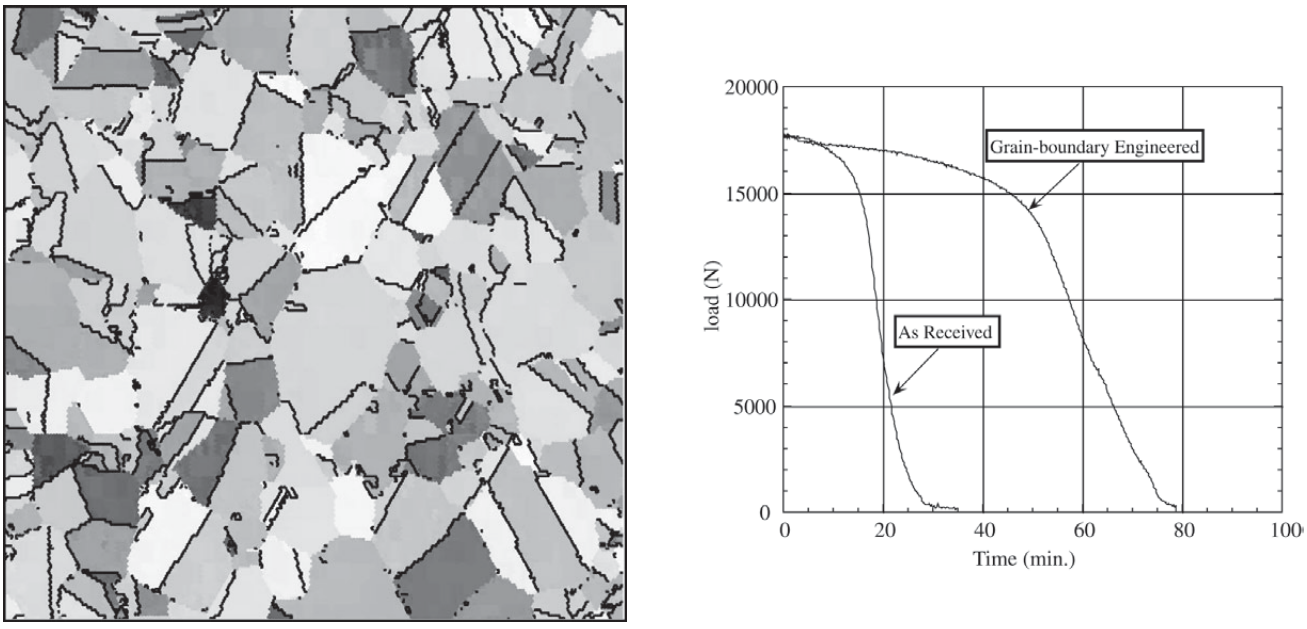

(a) (b)

Figure 7. a) OIM^TM mapping of a GBE-processed specimen; b) cracking of IN718 4pt-bending specimens in the as-received and in the GBE-processed condition.

the GB diffusivity depends on the structure of the GB[22]. The GB diffusivity has minimum values for special GBs, i.e., GBs with a high fraction of coincidence lattice sites between the neighboring grains ($\Sigma \leq 29$, Σ is the reciprocal value of the fraction of coincidence lattice sites).

To obtain specimens with an increased fraction of special GBs, a part of the IN718 material was thermo-mechanically processed (GBE). Similar to the results obtained in several earlier studies (e.g., in[24]) the fraction of special GBs (Σ 3-Σ 29) could be increased from 20.9% (as-received) to 41% (GBE). Figure 7a shows as an example the orientation mapping for the GBE condition, where the black lines indicate special GBs. Fixed-displacement tests were carried out on both as-received and grain-boundary-engineered bending specimens. The two exemplary load drop *vs.* time curves in Fig. 7b show that a higher fraction of special GBs increased the incubation time (perhaps by lowering the creep rate) and decreased the maximum crack propagation rate from approx. da/dN=8 µm/s to da/dN=3 µm/s, which may be attributed to a higher resistance of special GBs against dynamic embrittlement due to their lower oxygen GB diffusivity.

In order to obtain detailed information about the interdependence between the crystallographic orientation and the dynamic-embrittlement mechanism, IN718 bicrystals with defined misorientation relationships have been produced. Figure 8 shows one of the preliminary results of four-point bending tests under fixed-displacement loading. The load drop vs. time curve for oxygen-induced fracture of a Σ 5 tilt boundary clearly demonstrates that crack propagation is a continuous process and that no obvious incubation time is required; i.e., crack propagation sets in as soon as oxygen diffuses into the GB.

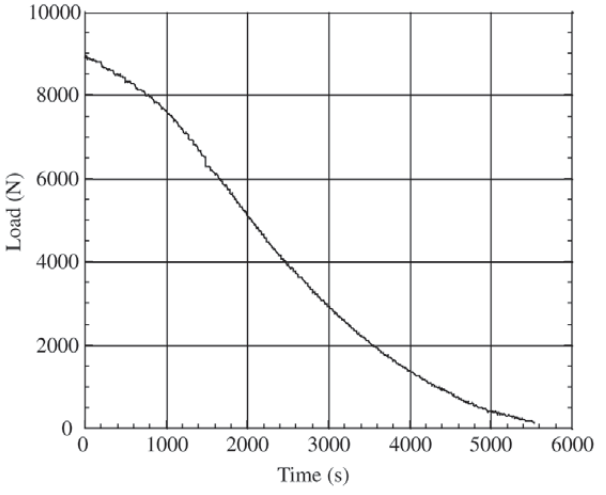

Figure 8. Load drop *vs.* time for cracking of a Σ 5 GB under fixed displacement at 650 °C.

The comparison with several other special and random GB and the application of the steady state model mentioned in Section 3 is the subject of ongoing work and will provide quantitative information about the influence of the misorientation relationship on the dynamic embrittlement mechanism and the grain boundary diffusion coefficient of oxygen in Ni base superalloys.

6. Conclusions

Atmospheric oxygen can cause a strong deterioration of the mechanical properties of polycrystalline Ni-base superalloys. At temperatures above 600 °C the oxygen GB diffusivity becomes fast enough to cause a transition from transgranular to brittle intergranular fracture during slow fatigue as well as static loading conditions. Several authors have attributed this transition to grain boundary oxidation. However, four-point bending tests under fixed displacement on IN718 specimens carried out during the present study provide some evidence that short-range GB diffusion of oxygen leading to GB decohesion (dynamic embrittlement) might be the governing mechanism for intergranular fracture at high temperature. GB diffusion depends to some extent on the structure of the grain boundaries. Particular GBs with a high fraction of coincident lattice sites (special GBs) exhibit low GB diffusivities. In agreement with this, the resistance against oxygen-induced intergranular fracture could be improved by grain-boundary engineering processing, i.e., by a sequence of several cold rolling and annealing steps that resulted in a 100% increase of special GBs.

Acknowledgements

This work is funded by the U.S. Air Force Office of Scientific Research under grant no. 538532, by the U.S. Department of Energy, Basic Energy Sciences, under grant no. DE-FGO-OIER 45924, and by the Alexander von Humboldt Foundation through a Feodor Lynen fellowship to UK, which is gratefully acknowledged.

References

1. Chang, K.-M.; Henry, M.F.; Benz, M.G. *JOM*, v. 12, p. 29, 1990.
2. Ghonem, H.; Nicholas, T.; Pineau, A. *Fatigue Fract. Engng. Mater. Struct.*, v. 16, p. 565, 1993.
3. Ghonem, H.; Nicholas, T.; Pineau, A. *Fatigue Fract. Engng. Mater. Struct.*, v. 16, p. 577, 1993.
4. Molins, R.; Hochstetter, G.; Chassaigne, J.C.; Andrieu, E. *Acta Mater.,* v. 45, p. 663, 1997.
5. Ghonem, H.; Zheng, D. *Mater. Sci. Eng.*, v. A150, p. 151 1992.
6. Pedron, J.P.; Pineau, A. *Mater. Sci. Eng.*, v. 56, p. 143, 1982.
7. Rösler, J.; Müller, S. *Scripta Mater.*, v. 40, p. 257, 1998.
8. Krupp, U.; Kane, W.M.; Düber, O.; Laird, C.; McMahon Jr., C.J. *Mater. Sci. Eng.* v. A349, p. 213, 2003.
9. Carpenter, W.; Kang, B.S.J.; Chang, K.-M. *Proc. Superalloys 718*,625,706 and *Various Derivates*, M. Loria (Ed.) The Minerals, Metals & Materials Society, p. 679-688, 1997.
10. McMahon Jr., C.J.; *Mater. Sci. Eng.*, v. 13, p. 295 (1970)
11. Andrieu, E.; Pieraggi, B.; Gourgues, A.F. *Scripta Mater.*, v. 4/5, p. 597, 1998.
12. Hull, D.; Rimmer, D.E. *Phil. Mag.*, v. 4, p. 673, 1959.
13. Bika, D.; Pfaendtner, J.A.; Menyhard,M.; McMahon Jr., C.J. *Acta Met. Mat.*, v. 43, p. 1895, 1995.
14. Muthiah, R.C.; Pfaendtner, J.A.; Ishikawa, S.; McMahon Jr., C. J. *Acta Mater.*, v. 47, p. 2797, 1999.
15. Muthiah, R.C.; McMahon Jr., C.J.; Guha, A. *Mater. Sci. Forum*, v. 207-209, p. 585, 1996.
16. Dymek, S.; Wrobel, M.; Dollar, M. *Scripta Mater.*, v. 43, p. 343, 2000.
17. Liu, C.T.; White, C.L. *Acta Metall.*, v. 35, p. 643, 1987.
18. Pfaendtner, J.A.; McMahon Jr., C.J. *Acta Mater.*, v. 49, p. 3369, 2001.
19. Xu, Y.; Bassani, J.L. *Mater. Sci. Eng.*, v. A260, p. 48, 1999.
20. Suresh Babu, V.; Pavlovic, A.S.; Seehra, M.S. *Proc. Superalloys 718*,625,706 and *Various Derivates*, M. Loria (Ed.) The Minerals, Metals & Materials Society, p. 689-693, 1997.
21. Connoley, T.; Reed, P.A.S.; Starink, M.J. *Mater. Sci. Eng.*, in press.
22. Diboine, A.; Pineau, A. *Fatigue Fract. Engng. Mater.* Struct., v. 10, p. 141, 1987.
23. Mishin, Y.; Herzig, C. *Mater. Sci. Eng.*, v. A260, p. 55, 1999.
24. Watanabe, T.; King, W.E. *Acta Mater.*, v. 47, p. 4171, 1999.